these sites, and the first month of full operations yielded a duty cycle of 89%. The first diurnal side lobe has been reduced by a factor of 280 in power (Fig. 2B).

The GONG Instrument and Data Reduction

The GONG instrument (*10*) was designed to observe the Doppler shift of the solar absorption line of Ni i (at wavelength 676.8 nm) primarily for *p* modes. Doppler velocity measurements were chosen because they typically have a higher ratio of the oscillatory signal compared to other solar processes. The actual measurement is of the phase of the single strongest (on average) Fourier component in a small portion of the spectrum around one absorption line. Such instruments are known in the solar community as "Fourier tachometers" (*11*). In the optics community, the basic technique is known as phase-shift interferometry and is widely used to test the quality of optical components. All of the instrumental design goals have been met or exceeded; in particular, the noise level of the measurements is two orders of magnitude below the noise generated by nonoscillatory solar processes.

Each minute, a single site records three 256-pixel by 242-pixel images, a total of 393 kilobytes of information. On average, 1.8 sites observe concurrently, so the average total data rate for the network is over 1 gigabyte per day. In order to maintain cadence, data must be reduced and archived at the same overall rate as they are collected. Many of the processing steps are independent, so the computational burden has been distributed over a network of workstations. This approach allows parallel processing of several steps and allows data reduction to maintain cadence with the data collection (*12*).

The images are processed, filtered, calibrated, and converted to Doppler velocity, modulation (approximate line strength), and total intensity images (*13*). The spherical harmonic decomposition of each remapped image is estimated up to $\ell = 250$ (*14*), thereby sampling all of the globally resonant modes. Time series of the mode amplitudes obtained simultaneously at different sites are corrected and combined (*15*), and the power spectra are computed. Finally, the frequencies, amplitudes, and linewidths of peaks in the power spectra are estimated (*16*). These parameters are then used to infer the solar internal conditions. The GONG network will provide this information for at least the next 3 years.

REFERENCES AND NOTES

1. The original papers providing the theoretical underpinnings of the oscillations are R. Ulrich, *Astrophys. J.* **162**, 993 (1970); J. W. Leibacher and R. F. Stein, *Astrophys. Lett.* **7**, 191 (1971); C. L. Wolff, *Astrophys. J.* **177**, L87 (1972). For more recent reviews of the subject, see D. O. Gough and J. Toomre, *Annu. Rev. Astron. Astrophys.* **29**, 627 (1991); A. N. Cox, W. C. Livingston, M. S. Matthews, Eds., *Solar Interior and Atmosphere* (Univ. of Arizona Press, Tucson, 1991), pp. 329–660; W. Unno, Y. Osaki, H. Ando, H. Saio, H. Shibahashi, *Nonradial Oscillations of Stars* (Univ. of Tokyo Press, Tokyo, 1989).
2. J. W. Harvey, *AIP Conf. Proc.* **189**, 227 (1989).
3. P. H. Scherrer *et al.*, *Sol. Phys.* **162**, 129 (1995).
4. Y. Elsworth *et al.*, *Astron. Soc. Pac. Conf. Ser.* **76**, 392 (1995).
5. E. Fossat, *Sol. Phys.* **133**, 1 (1991).
6. D. Y. Chou *et al.*, *ibid.* **160**, 237 (1995).
7. E. J. Rhodes Jr. *et al.*, *Astron. Soc. Pac. Conf. Ser.* **76**, 398 (1995).
8. F. Hill and G. Newkirk Jr., *Sol. Phys.* **95**, 201 (1985).
9. F. Hill *et al.*, *ibid.* **152**, 321 (1994); *ibid.*, p. 351.
10. J. W. Harvey *et al.*, in preparation.
11. J. Beckers and T. M. Brown, *Oss. Mem. Oss. Astrofis. Arcetri* **106**, 189, (1978).
12. F. Hill *et al.*, in preparation.
13. R. Toussaint, J. W. Harvey, R. P. Hubbard, *Astron. Soc. Pac. Conf. Ser.* **76**, 532 (1995).
14. T. Brown, in *Advances in Helio- and Asteroseismology*, J. Christensen-Dalsgaard and S. Frandsen, Eds. (Reidel, Dordrecht, 1988), pp. 453–465.
15. The time series from each site-day, scaled to compensate for variations in image resolution from seeing and other effects, are merged to form a longer, more nearly continuous time series. The uncertainty in the scaling estimate is used as a measure of data quality to weight the time series [W. Williams, F. Hill, C. Toner, T. Brown, *Astron. Soc. Pac. Conf. Ser.* **42**, 441 (1993); W. Williams, F. Hill, C. Toner, *ibid.* **52**, 494 (1993); W. Williams, C. Toner, F. Hill, *ibid.* **76**, 500 (1995); in *Fourth SOHO Workshop: Helioseismology Volume 2*, J. T. Hoeksema, V. Domingo, B. Fleck, B. Battrick, Eds. (European Space AgencyPubl. Div., Noordwijk aan Zee, Netherlands, 1995), pp. 185–189]. Merging algorithms have also been developed in the context of nonimaged helioseismology for the IRIS network [E. Fossat, *Astron. Astrophys.* **263**, 443 (1992)].
16. F. Hill *et al.*, *Science* **272**, 1292 (1996).

17. The GONG project is managed by the National Solar Observatory, a Division of the National Optical Astronomy Observatories, which is operated by the Association of Universities for Research in Astronomy under a cooperative agreement with NSF.

18 March 1996; accepted 6 May 1996

The Current State of Solar Modeling

J. Christensen-Dalsgaard, W. Däppen, S. V. Ajukov, E. R. Anderson, H. M. Antia, S. Basu, V. A. Baturin, G. Berthomieu, B. Chaboyer, S. M. Chitre, A. N. Cox, P. Demarque, J. Donatowicz, W. A. Dziembowski, M. Gabriel, D. O. Gough, D. B. Guenther, J. A. Guzik, J. W. Harvey, F. Hill, G. Houdek, C. A. Iglesias, A. G. Kosovichev, J. W. Leibacher, P. Morel, C. R. Proffitt, J. Provost, J. Reiter, E. J. Rhodes Jr., F. J. Rogers, I. W. Roxburgh, M. J. Thompson, R. K. Ulrich

Data from the Global Oscillation Network Group (GONG) project and other helioseismic experiments provide a test for models of stellar interiors and for the thermodynamic and radiative properties, on which the models depend, of matter under the extreme conditions found in the sun. Current models are in agreement with the helioseismic inferences, which suggests, for example, that the disagreement between the predicted and observed fluxes of neutrinos from the sun is not caused by errors in the models. However, the GONG data reveal subtle errors in the models, such as an excess in sound speed just beneath the convection zone. These discrepancies indicate effects that have so far not been correctly accounted for; for example, it is plausible that the sound-speed differences reflect weak mixing in stellar interiors, of potential importance to the overall evolution of stars and ultimately to estimates of the age of the galaxy based on stellar evolution calculations.

Stars are born from contracting interstellar clouds. The initial rapid phases of evolution are rather uncertain; however, the protostar eventually settles down to a state where the forces of gravity and the pressure gradient approximately balance. The continuing contraction releases gravitational energy, which heats up the stellar matter and supplies the luminosity of the early star. Eventually, the temperature in the stellar core gets sufficiently high that the energy released in the fusion of hydrogen into helium begins to contribute to the luminosity. Contraction stops when fusion produces all of the luminosity. The star then enters the very long main-sequence phase, during which essentially all of the hydrogen in the core is gradually converted into helium. This phase occupies the largest fraction of its life, lasting about 10 billion years in the solar case.

So far, the sun has used up about half of its hydrogen supply. When the hydrogen at the center is exhausted, in about 5 billion years, fusion will continue in a shell around the helium core. During this phase, the sun will expand greatly, becoming finally a red giant. The sun will end as a white dwarf, comprising much of the original mass but with a radius similar to that of the Earth.

In general, a protostellar cloud is likely to be in some state of rotation, which is greatly amplified during the contraction phase. The spin-down to the present state of slow solar internal rotation, as helioseismically inferred (*1*), may have involved material motion or instabilities, leading to mixing in the solar interior and thus affecting the structure of the present sun; however, the modeling of these processes is currently uncertain (*2*).

Modeling the Sun: Macro- and Microphysics

The details of solar evolution have been filled in by means of numerical calculations of solar models. When describing the ingredients in such calculations, it is convenient to distinguish between "macrophysics" and "microphysics." The latter defines the detailed physical properties of matter in the sun. Here we discuss the macrophysics, defined as the larger scale aspects of solar structure, and the assumptions involved in what might be called standard solar modeling (*3*).

The structure of a star is a result of a balance of forces, a balance between the energy loss at the stellar surface and energy generation in the core, and stationary energy transport between the core and the surface. The balance of forces, described as hydrostatic equilibrium, provides a relation between the pressure gradient and the gravitational acceleration. The force of gravity is determined by the density distribution in the star; thus, we must relate density to pressure (*4*) through the properties of the matter and hence the microphysics. More specifically, the relevant properties of stellar matter are expressed by the equation of state, connecting pressure p, density ρ, temperature T, and composition. The latter is often characterized by the fractional mass abundances X, Y, and Z of hydrogen, helium, and heavier elements, respectively.

The temperature of the stellar interior is determined by the energy balance. In much of the sun, energy transport takes place by means of radiation and depends on atomic absorption coefficients, which determine the opacity of stellar matter (*5*). It was also realized early on that radiative transport may require a temperature gradient so steep as to lead to convective instability (*6*); convection then generally dominates the energy transport. In the sun, this process occurs in the outer 30% of the radius (*7*). Because of the efficiency of convective energy transport, it generally requires a temperature gradient only slightly steeper than adiabatic; then pressure and density are approximately related by $p \simeq K\rho^{\gamma_1}$, where K is a constant and $\gamma_1 = (\partial \ln p/\partial \ln \rho)_{ad}$, the derivative corresponding to an adiabatic change (that is, one occurring without heat exchange). The temperature gradient substantially exceeds the adiabatic value only near the surface (*8*), in a thin region that determines K; in the commonly used mixing-length formalism, K is controlled by a parameter that measures convective efficiency (*9*).

In standard solar models, it is assumed that the solar luminous output derives from the fusion of hydrogen into helium (*10*). The conservation laws of particle physics dictate that the production of one helium nucleus leads to the emission of two neutrinos. Thus, measurements of the flux of neutrinos from the sun can in principle test the properties of solar nuclear energy generation. Such measurements have yielded values substantially below those predicted by standard solar models; this deficit is the long-standing solar neutrino problem (*11*).

The life history of a star is intimately related to changes in its composition. These changes can be followed numerically with sequences of models (*12*), starting either during the contraction phase or from a state of chemical homogeneity. The largest changes in composition result from the fusion of hydrogen into helium; however, changes in the chemical distribution of elements as a result of gravitational settling also play a significant role in determining the structure of the present sun (*13*).

A viable model of the present sun, of one solar mass and at the inferred solar age, should have the proper radius and luminosity, as well as the observed surface ratio of heavy elements to hydrogen. These basic properties can be determined fairly accurately: the mass is $M_\odot = 1.989 \times 10^{33}$ g, the solar radius is $R_\odot = 6.96 \times 10^{10}$ cm, and the solar luminosity is $L_\odot = 3.846 \times 10^{33}$ erg s^{-1} (*14*). The chemical composition is known from spectroscopic observations, with the important exception of helium; the present surface abundance yields an abundance ratio between heavy elements and hydrogen of $Z/X = 0.0245 \pm 0.005$ (*15*). The age of the sun, since the onset of core hydrogen burning, is estimated at $(4.52 \pm 0.04) \times 10^9$ years (*16*). The correct values of the radius and luminosity can be obtained by adjusting the initial helium abundance and a parameter characterizing the near-surface convection (*17*). Also, the initial heavy-element abundance is generally chosen to obtain the observed surface value in the model of the present sun.

Given the microphysics, the preceding description provides a well-defined procedure for computing standard models in accordance with the known overall properties of the sun. On the other hand, it involves several significant simplifications, which might compromise the resulting models. It neglects possible macroscopic motion in the solar interior, which would change the composition profile; such motion might result from instabilities associated with the slowdown of rotation or convective overshoot into the stable region beyond the base of the convection zone (*18*). Also, it neglects large convective velocities just below the top of the convection zone, which give rise to a turbulent pressure contributing as much as 10% of the total pressure (*19*). Finally, it neglects mass variations even though mass loss or accretion may have taken place during the core hydrogen-burning phase of solar evolution (*20*).

The discrepancy between the predicted and measured neutrino fluxes could in principle indicate problems with the standard models. Also, although the solar distribution among the heavy elements is typically similar to the composition of the early solar system as estimated from meteoritic abundances, lithium is depleted by a factor of about 150 relative to the estimated initial abundance, and beryllium is also somewhat lacking (*15*). This depletion is likely to have been caused by nuclear burning, which, in the case of lithium, requires mixing down to a temperature of around 2.6×10^6 K. Yet, in standard solar models the temperature never reaches this value at the base of the convection zone, and the predicted depletion of lithium is at most a factor of 4 (*21*). Thus, the observed low lithium abundance is evidence either for mixing well beyond the convection zone at

J. Christensen-Dalsgaard and S. Basu are with Theoretical Astrophysics Center and Institute of Physics and Astronomy, Aarhus University, DK-8000 Aarhus C, Denmark. W. Däppen and E. J. Rhodes Jr. are with the Department of Physics and Astronomy, University of Southern California, Los Angeles, CA 90089, USA. S. V. Ajukov is with the Sternberg Astronomical Institute, Moscow, Russia. E. R. Anderson, J. W. Harvey, F. Hill, and J. W. Leibacher are with the National Solar Observatory, National Optical Astronomy Observatories, Tucson, AZ 85726, USA. H. M. Antia and S. M. Chitre are with the Tata Institute of Fundamental Research, Bombay, India. V. A. Baturin, I. W. Roxburgh, and M. J. Thompson are with the Astronomy Unit, Queen Mary and Westfield College, London E1 4NS, UK. G. Berthomieu, P. Morel, and J. Provost are with the Observatoire de la Côte d'Azur, Nice, France. B. Chaboyer is with CITA, University of Toronto, Toronto, Canada. A. N. Cox and J. A. Guzik are with Los Alamos National Laboratory, Los Alamos, NM 87545, USA. P. Demarque is with the Department of Astronomy, Yale University, New Haven, CT 06520, USA. J. Donatowicz and G. Houdek are with the Institut für Astronomie, Universität Wien, Vienna, Austria. W. A. Dziembowski is with the Copernicus Center, Warsaw, Poland. M. Gabriel is with the Institut d'Astrophysique, Université de Liège, Liège, Belgium. D. O. Gough is with the Institute of Astronomy, University of Cambridge, Cambridge, UK. D. B. Guenther is with the Department of Astronomy and Physics, Saint Mary's University, Halifax, Nova Scotia, Canada. C. A. Iglesias and F. J. Rogers are with the Lawrence Livermore National Laboratory, Livermore, CA 94550, USA. A. G. Kosovichev is with Center for Space Science and Astrophysics, Stanford University, Stanford, CA 94305, USA. C. R. Proffitt is with Computer Sciences Corporation, Goddard Space Flight Center, Greenbelt, MD 20771, USA. J. Reiter is with the Mathematisches Institut, Technische Universität München, Munich, Germany. R. K. Ulrich is with the Department of Physics and Astronomy, University of California, Los Angeles, CA 90095, USA.

some stage of solar evolution or for mass loss to an extent sufficient to expose depleted material. As a reference standard solar model, we use Model S, computed with the global parameters described above (22).

Some Properties of Solar Oscillations

Models of solar evolution must be checked against observations. The extensive and accurate measurements of the solar 5-min oscillations provide key tests of even subtle features of the models. The solar 5-min oscillations (23) consist of a large number of modes that each extend in the radial direction from the surface to the inner turning point, whose distance r_t from the solar center is a function of $\nu/(\ell + 1/2)$, where ν is the frequency and ℓ is the degree of the mode. Modes of low degree penetrate almost to the center of the sun (Fig. 1), whereas higher degree modes are trapped closer to the surface. The modes observed with the GONG network, of degree between 0 and about 250, span a range in r_t between the center and $0.98R_\odot$, essentially permitting resolution of solar structure and rotation throughout this range (1, 24).

In almost the entire solar interior, the thermal time scale is so long, compared with the periods of oscillation, that the oscillations can be regarded as adiabatic. Thus, the relative perturbations in pressure and density, when following the motion, are related by the adiabatic exponent γ_1. To the extent that this relation holds, the oscillations are purely mechanical, with frequencies determined by the variation of p, ρ, and γ_1 with radius. The adiabatic approximation breaks down near the surface. Here the full energy equation for the oscillations must be considered, including the perturbation in the radiative flux and the highly uncertain perturbation in the convective flux; thus, although nonadiabatic calculations may indicate the magnitude of the resulting effects on the frequencies, a detailed application to the analysis of the observations is not yet possible (25).

Here we consider only adiabatic oscillations and generally treat convection according to the simple mixing-length prescription, neglecting effects of turbulent pressure; it is then straightforward to compute numerically precise frequencies for a given solar model (26). Although the approximations undoubtedly introduce errors in the treatment of the model and oscillations in the near-surface region, it is possible to analyze the observed frequencies in a way that largely separates the likely effects of these errors from those of errors in deeper parts of the model. The near-surface effects on the frequencies have two properties: they depend on frequency because of the detailed nature of the mode in this region, and they depend on the turning-point position, because modes trapped near the surface involve a smaller part of the sun, and hence are easier to perturb, than modes penetrating to the deep interior. The latter effect can be eliminated by suitable scaling with the mode inertia (27). It appears that near the surface, the properties of the modes depend little on degree (Fig. 1); so, therefore, does the influence of the near-surface effects (28).

Frequency differences (Fig. 2A) between models using alternative treatments of the upper part of the convection zone and those using the normal mixing-length treatment show that the scaled difference is indeed a function of frequency alone. The differences (Fig. 2B) between the GONG mean frequencies and frequencies of the reference Model S largely share the same property. This result confirms that the dominant components in the model errors belong to the near-surface region. Although the nature of the errors is uncertain, their effect has roughly the same magnitude and frequency dependence as those illustrated in Fig. 2A.

A closer look at the frequency differences in Fig. 2B reveals a division into two branches, suggesting that there is also a dependence on the depth of penetration of the modes. If one subtracts a smooth function of frequency fitted to the data and plots the residual against the turning-point radius r_t (Fig. 2C), there is a sharp jump in the residuals at an r_t that corresponds to the region just below the convection zone. Inversion of the frequency differences does indeed reveal a localized sound-speed difference at this point (24).

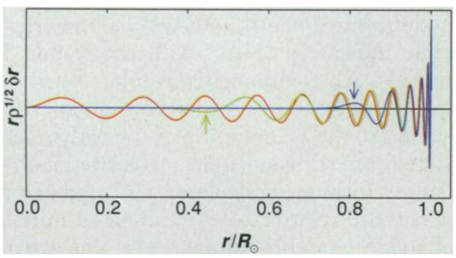

Fig. 1. Radial variation of the eigenfunction for three modes of similar frequency ν but differing degree ℓ. The red curve shows a mode of degree $\ell = 0$ and frequency $\nu = 3310$ μHz, the green curve is for $\ell = 20$, $\nu = 3375$ μHz, and the blue curve is for $\ell = 70$, $\nu = 3405$ μHz. The quantity plotted reflects the distribution of energy in the modes and hence their sensitivity to solar structure. The arrows indicate the locations of the asymptotic turning points r_t, determined by the frequency ν and ℓ from the relation $c(r_t)/r_t = 2\pi\nu/(\ell + 1/2)$ (63), c being the adiabatic speed of sound.

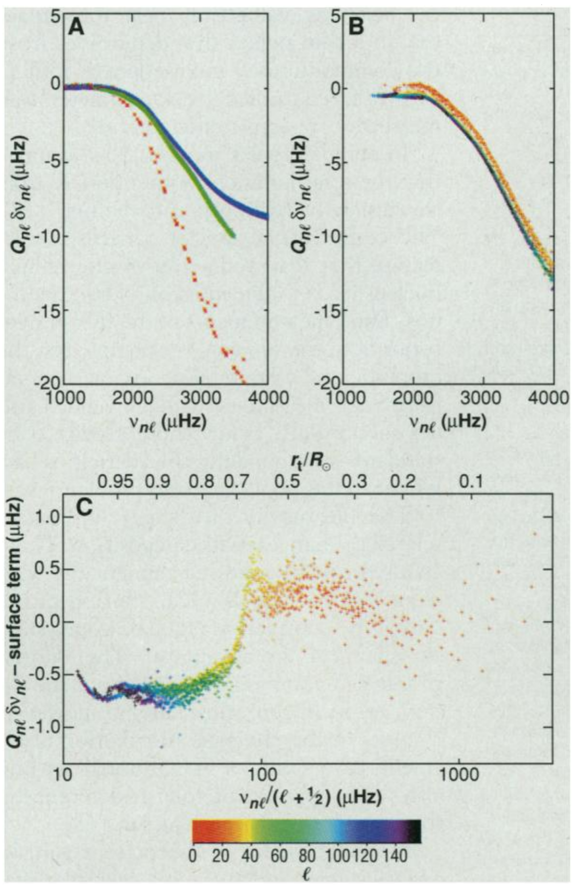

Fig. 2. Frequency differences scaled by $Q_{n\ell} = E_{n\ell}/\bar{E}_0(\nu_{n\ell})$, where $\bar{E}_0(\nu)$ is the inertia of radial modes, interpolated to the frequency ν (27). (**A**) Differences for three modifications of the near-surface region of solar models, relative to a normal mixing-length model: blue points result from an alternative treatment of the convective flux (64); green points are based on inclusion of turbulent pressure (65); and for the red points, the uppermost parts of the convection zone were represented by an averaged hydrodynamical simulation (66). (**B**) Differences between GONG observed frequencies and frequencies of the reference Model S. (**C**) Differences in panel (B), after subtracting a smooth fit to the frequency-dependent component. The residuals have been plotted against $\nu/(\ell + 1/2)$, which is directly related to the turning-point radius r_t of the mode. In (B) and (C), the degree ℓ is indicated by the color bar.

Properties of the Solar Plasma

The aspects of the microphysics most accessible to helioseismic investigation are the equation of state and opacity. The interior of the sun is a plasma: it is essentially neutral close to the photosphere, becomes partially ionized in roughly the outer 20,000 km, and is nearly fully ionized from there down to the center. The high accuracy of helioseismic data carries the promise of probing the properties of this plasma under conditions that have not yet been achieved in the laboratory. In the absence of experimental data, solar models are based on theoretical calculations of the equation of state and opacity, which can then be tested against the helioseismic data.

The simplest model is that of a mixture of fully ionized nuclei and electrons obeying the perfect gas law. However, an ideal equation of state can be more general by including deviations from the perfect gas law, due to ionization, radiation, and degenerate electrons (*29*). Departures from ideality arise from dynamical interactions between the components of the plasma. One measure of the nonideality is the ratio between the average potential energy resulting from the Coulomb interaction and the kinetic energy of particles (*30*). Although the solar plasma is only slightly nonideal, the deviations from nonideality can be studied in detail because of the observational constraints afforded by helioseismology.

The equation of state. There are two basic approaches to realize nonideal equations of state: the so-called chemical and physical pictures. In the chemical picture, one assumes that the notion of atoms and ions still makes sense, and ionization is treated like a chemical reaction (*31*). A simple example is the EFF (Eggleton-Faulkner-Flannery) formulation (*32*), which has seen widespread use in stellar modeling. One of the more recent realizations is the Mihalas-Hummer-Däppen (MHD) equation of state, in which modifications of atomic states are expressed in a heuristic and intuitive way, by the probability that the state is occupied as a function of the parameters of the surrounding plasma (*33*).

The physical picture provides a systematic method to include nonideal effects. An example is the equation of state underlying the OPAL opacity project (*34*). It starts out from the grand canonical ensemble of the basic constituents (electrons and nuclei) of a system interacting through the Coulomb potential. Configurations corresponding to bound combinations of electrons and nuclei, such as ions, atoms, and molecules, arise naturally as terms in cluster expansions. Any effects of the plasma environment on the internal states are obtained directly from the statistical-mechanical analysis, rather than by assertion as in the chemical picture (*35*).

The first obvious nonideal effect is a direct result of the Coulomb force between charged particles. Because of the long-range nature of the Coulomb force, this effect is usually described as a screening of the positive charges by surrounding electrons. It corresponds to an effective attraction between particles. Another nonideal effect results from the interaction between bound particles and is commonly referred to as pressure (or density) ionization. These nonideal effects have to be included in an equation of state of helioseismic precision. Simple equations of state fail to account for pressure ionization because they usually do not assign a radius to atoms and ions, thus allowing recombination at high densities, such as those found in the solar center (*36*). Only by treating atoms and ions as extended species can the spurious recombinations be prevented. Even so, a significant fraction of He^+ ions might in principle survive at the solar center (*37*), which could affect solar structure at a level detectable by helioseismology.

Helioseismology may probe important effects of the equation of state through the decrease in γ_1 caused by ionization, particularly in the second ionization zone of helium (lying at a depth of about 15,000 km), which is sufficiently deep to be largely unaffected by the near-surface uncertainties (*38*). Here the response of γ_1 to ionization provides a test of the equation of state and a measure of the helium abundance $Y_\odot$ in the solar convection zone. Determinations of $Y_\odot$ are sensitive to uncertainties in the equation of state; recent values tend to be around $Y_\odot \simeq 0.24$ (*39*).

Helioseismology has clearly shown the effect of the leading-order Coulomb correction in the solar data (*40*). The differences between sound speed calculated with the EFF and MHD equations of state are only a few percent (Fig. 3A, red, solid lines); they closely reflect the changes in γ_1, which in turn is intimately linked to the ionization processes in the gas. The resulting frequency differences (Fig. 3B) are huge, compared with the intrinsic accuracy of the observations [see figure 3 of (*41*)]. It is this sensitivity that made immediately obvious the improvements resulting from the inclusion of Coulomb effects.

Beyond the first-order contribution, things become much more subtle. The leading-order correction overestimates the whole Coulomb-pressure effect; at sufficiently high density, it causes the total gas pressure to become nonsensically negative. Chemical-picture equations of state, such as

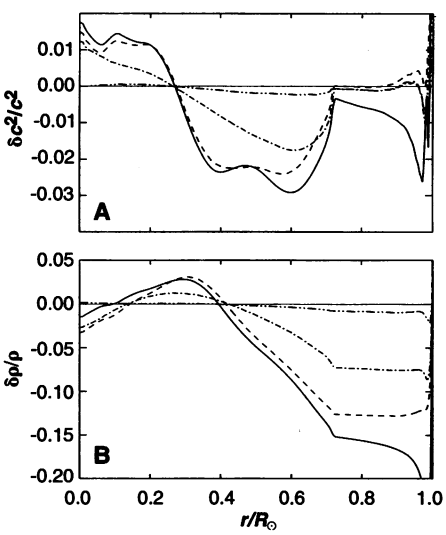

Fig. 4. Differences relative to the reference Model S of (**A**) squared sound speed c^2 and (**B**) density ρ in four models based on various approximations to the physics. Solid lines: EFF equation of state (*32*) with Cox and Tabor opacities (*44*). Dashed lines: MHD equation of state (*33*) with Cox and Tabor opacities. Dot-dashed lines: MHD equation of state with OPAL opacities (*34*). Double-dot-dashed lines: MHD with OPAL opacities again, but including settling of helium and heavy elements.

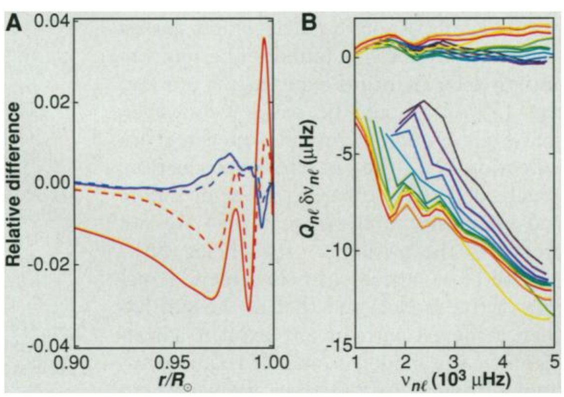

Fig. 3. (**A**) Relative differences, at fixed radius, in γ_1 (dashed curves) and squared sound speed (solid curves) between two pairs of models: red, a model computed with the EFF equation of state (*32*) minus a model computed with the MHD formulation (*33*); blue, differences between a model computed with the OPAL equation of state (*34*) and the MHD model. (**B**) Corresponding frequency differences between the EFF and MHD models (lower set of curves) and the OPAL and MHD models (upper set) for modes of degree 0, 20, . . . , 200. Points of the same degree have been connected by lines coded in color according to the color bar in Fig. 2.

MHD, need a switch-off device to prevent negative pressures. In contrast, the OPAL equation of state does not suffer from such problems: it contains systematic terms beyond the leading-order Coulomb correction.

The differences between the MHD and OPAL equations of state (Fig. 3) are much smaller than those for the EFF case, reflecting the fact that both MHD and OPAL contain the leading Coulomb effects. However, the frequency changes are still much higher than the observational uncertainty; although simple inspection of frequency differences between observations and models do not reveal the effects of the equation of state at this level of detail, such effects are quite evident in more sophisticated analyses (*42, 43*). These reveal, for example, that MHD is superior to a simpler formulation involving just the Coulomb correction to the EFF equation of state. Also, there is some evidence from sound-speed inversion that the OPAL equation of state provides a better fit to the sun than MHD.

Opacity. The opacity of stellar material controls the energy flow through a star and ultimately its luminosity. Early opacity calculations were based on hydrogenic approximations and related simplifications of the physics (*44*). From the beginning of the 1970s, it was noticed that some problems with the calculated properties of variable stars, particularly period ratios of Cepheid stars, could be solved by increasing the interior opacity (*45*). As a result, two opacity efforts using quite different approaches were undertaken. The OPAL group showed that earlier opacities grossly underestimated the bound-state contribution from iron; the improvements led to the increase of the total opacity required to model Cepheid stars successfully (*46*). Results from the parallel Opacity Project (*47*) are in surprisingly good agreement with OPAL, providing a level of confidence. Introduction of these new opacities has led to the solution of a number of long-standing difficulties in modeling stars and stellar pulsations (*48*), without introducing problems.

Before the new opacity results were available, it was noted that a modest increase of 10 to 20% in the opacity just below the bottom of the convection zone could improve the agreement of calculated p-mode frequencies with solar observations (*49*). Such an enhancement of the opacity in this region was obtained by OPAL, mainly as a result of the effect of the improved equation of state on the ion balance, and led to substantial improvements in the agreement with helioseismic data (*50*).

The calculations have increased the opacity for the solar center, requiring an increase in initial helium abundance from about 0.24 to about 0.27 to calibrate the model (*51*). Interestingly, in models with helium settling, this enrichment results in a present surface helium abundance of around 0.24, roughly consistent with the helioseismically inferred values (*39*). We note, however, that there is a recent controversy about collective plasma corrections to the solar-center opacity (*52*).

Progress in Solar Modeling

In the last decade there have clearly been major efforts directed toward improvements in the physics of the solar interior. To illustrate their effect on models of the sun, Fig. 4 shows relative differences between models computed with various approximations to the physics and the reference Model S. The latter model appears to be a relatively good approximation to the sound-speed and density structure of the sun (*24*). Four models are shown, differing in the equation of state and capacity relations, and whether or not gravitational settling was included. It is evident that the MHD equation of state improves the sound speed in the convection zone. Also, the OPAL opacities substantially improve the structure of the radiative interior, as does the inclusion of gravitational settling; indeed, it is striking that the latter effect is as large as that resulting from use of the OPAL tables rather than those of Cox and Tabor (*53*). To put these differences in perspective, we note that according to the inversions in (*24*), c^2 in Model S differs from that observed for the sun by no more than 0.5%, and the error in the model's density is below 2%.

Model S shares with other standard solar models predicted fluxes of solar neutrinos in substantial excess of the measured values (*11*). This excess might suggest that no solution of the neutrino problem can be found by modifying the computation of solar models while at the same time preserving agreement with the helioseismic data, thus perhaps strengthening the case for a solution involving the properties of the neutrinos (*54*). There are also arguments independent of the details of solar models which suggest that new physics is required if the four operating solar neutrino experiments are correct (*55*). It should be realized, however, that helioseismology provides no direct information on the neutrino production, which depends primarily on temperature and composition: these quantities are not probed by the oscillation frequencies (*56*).

The close agreement between the structure of the models and that of the sun has been achieved without any explicit adjustments of the models to match the observations, although much of the improvement in the physics has been motivated by the availability of the highly precise helioseismic data. Rather, the agreement results from incorporation of the best current description of the properties of the solar interior, including gravitational settling. Such agreement is a striking demonstration of our ability to model at least the gross features of the interior of a star. It is interesting that the improvements have taken place solely in the microphysics. However, Fig. 2C and the recent GONG results (*24*) demonstrate that there remain subtle differences, indicating the existence of physical effects that have not been taken into account. Although these differences arise in part from remaining inadequacies in the microphysics, it is tempting to speculate that we are also seeing effects of errors in the macrophysics and other simplifications of the calculations; a likely candidate is material mixing. Investigation of such effects will require full use of the data from helioseismic experiments such as GONG, combined with a wide range of investigations of properties of other stars. Particularly promising is the emerging possibility of extending seismic investigations to stars other than the sun (*57*).

REFERENCES AND NOTES

1. M. J. Thompson *et al.*, *Science* **272**, 1300 (1996).
2. Models of the evolution of solar internal rotation assume loss of angular momentum from the convection zone through the solar wind, the coupling to the interior taking place through various types of instability [A. S. Endal and S. Sofia, *Astrophys. J.* **243**, 625 (1981); M. H. Pinsonneault, S. D. Kawaler, S. Sofia, P. Demarque, *ibid.* **338**, 424 (1989)]. These models have been useful in interpreting rotational velocities and lithium abundances in stellar clusters and in field stars near the main sequence. When applied to the sun, they fail to reproduce the near-uniform rotation of the present solar interior, as inferred from helioseismology (*1*), indicating that other physical mechanisms must contribute to the solar internal spin-down.
3. The notion of "standard" models is an evolving concept; in a loose sense, such models should incorporate the physics that is generally recognized as relevant and for which an adequate theoretical description exists.
4. Simplified stellar models can be based on the condition of hydrostatic equilibrium and the assumption that pressure is related to density alone [for example, J. H. Lane, *Am. J. Sci. Arts 2nd Ser.* **50**, 57 (1870); R. Emden, *Gaskugeln* (Teubner, Leipzig, 1907)].
5. A substantial breakthrough in the physics of stellar interiors came with the treatment of radiative energy transport. On the basis of a relation between opacity and temperature gradient, the condition of hydrostatic equilibrium, and the equation of state, one can estimate the luminosity of a star without regard to the sources of energy. This procedure led A. S. Eddington [*The Internal Constitution of the Stars*, sect. 169 (Cambridge Univ. Press, Cambridge, 1926)] to consider the possibility that the sun consists primarily of hydrogen, contrary to the then prevailing view.
6. K. Schwarzschild, *Nachr. Königl. Ges. Wiss. Göttingen* **195**, 41 (1906).
7. The depth of the solar convection zone has been determined from helioseismic inversion to be (28.7 ± 0.3)% of the solar radius [J. Christensen-Dalsgaard, D. O. Gough, M. J. Thompson, *Astrophys. J.* **378**, 413 (1991); A. G. Kosovichev and A. V. Fedorova, *Astron. Zh.* **68**, 1015 (1991)].
8. Here the density is so low that convective velocities reaching a considerable fraction of the sound speed are required to sustain the flux of energy.
9. L. Biermann [*Z. Astrophys.* **5**, 117 (1932)] and T. G. Cowling [*Mon. Not. R. Astron. Soc.* **96**, 42 (1935)] were among the first to use mixing-length treatments

to describe the transport of energy by convection. For a refined version, now commonly used, see E. Böhm-Vitense, *Z. Astrophys.* **46**, 108 (1958); see (*58*) for an alternative, more recent formulation. Also, hydrodynamical simulations are now able to guide solar modelers [for example, R. F. Stein and Å Nordlund, *Astrophys. J.* **342**, L95 (1989); N. Brummell, F. Cattaneo, J. Toomre, *Science* **269**, 1370 (1995); Y.-C. Kim, P. A. Fox, S. Sofia, P. Demarque, *Astrophys. J.* **442**, 422 (1995)].

10. Early discussions of hydrogen fusion include C. F. von Weizsäcker, *Phys. Z.* **38**, 176 (1937); G. Gamow, *Phys. Rev.* **53**, 595 (1938); and H. A. Bethe, *ibid.* **55**, 434 (1939). The details of the processes dominating energy generation in the sun, in the so-called *pp* chains, were elucidated by J. B. Oke [*J. R. Astron. Soc. Can.* **44**, 135 (1950)]. Changes in the gravitational and internal energy, resulting from the fusion-induced changes of solar structure, also make a small contribution to the luminosity.
11. Neutrinos are detected by radiochemical reactions in ^{37}Cl and ^{71}Ga and by electron scattering in water, each experiment having a different response to the spectrum of neutrinos emitted by the sun. The ^{37}Cl and ^{71}Ga experiments yield neutrino capture rates of 2.3 and 78 solar neutrino units (SNU, defined as 1 capture per 10^{36} target atoms per second), respectively, and the electron scattering experiment yields a flux of the so-called ^{8}B neutrinos of 2.9×10^{6} cm^{-2} s^{-1}. The corresponding values predicted by Model S (*22*), which is typical of standard solar models, are 8.2 and 132 SNU and 5.9×10^{6} cm^{-2} s^{-1}, respectively. For further details on the neutrino problem, see J. N. Bahcall, *Neutrino Astrophysics* (Cambridge Univ. Press, Cambridge, 1989); H. Dzitko, S. Turck-Chièze, P. Delbourgo-Salvador, C. Lagrange, *Astrophys. J.* **447**, 428 (1995); and (*59*).
12. Early evolution calculations were carried out by C. B. Haselgrove and F. Hoyle [*Mon. Not. R. Astron. Soc.* **116**, 515 (1956)] and M. Schwarzschild, R. Howard, and R. Härm [*Astrophys. J.* **125**, 233 (1957)].
13. Although diffusion and settling were discussed by Eddington (*5*) and are unavoidable consequences of the normal assumptions of stellar modeling, their inclusion in detailed solar models is comparatively recent. See, for example, P. D. Noerdlinger, *Astron. Astrophys.* **57**, 407 (1977); P. Demarque and D. B. Guenther, *Advances in Helio- and Asteroseismology*, J. Christensen-Dalsgaard and S. Frandsen, Eds. (IAU Symp. 123, Reidel, Dordrecht, 1988), p. 91; and (*60*); C. R. Proffitt and G. Michaud, *Astrophys. J.* **380**, 238 (1991). The microscopic diffusion and settling rates were discussed by, for example, Michaud and Proffitt (*61*) and A. A. Thoul, J. N. Bahcall, and A. Loeb [*Astrophys. J.* **421**, 828 (1994)].
14. The mass of the sun is known from planetary motion, and the radius of the visible surface can be measured directly. The solar luminosity is inferred from space-based irradiance measurements [R. C. Wilson and H. S. Hudson, *Nature* **332**, 810 (1988)], assuming isotropic radiation and averaging over the solar-cycle variation of about 0.1% [for stellar evidence, see S. Baliunas and R. Jastrow, *Nature* **348**, 520 (1990)].
15. The abundances of elements other than helium can in general be determined with considerable precision [E. Anders and N. Grevesse, *Geochim. Cosmochim. Acta* **53**, 197 (1989); N. Grevesse and A. Noels, in *Origin and Evolution of the Elements*, N. Prantzos, E. Vangioni, M. Cassé, Eds. (Cambridge Univ. Press, Cambridge, 1993), p. 15]. Although helium was first detected in the solar spectrum, the formation of the helium lines is so complex that observation gives no precise information about its abundance.
16. The age of the sun can be estimated from the ages, obtained from radioactive dating, of the oldest meteorites. G. J. Wasserburg [in (*59*)] obtained a meteoritic age of $(4.57 \pm 0.01) \times 10^{9}$ years, and D. B. Guenther [*Astrophys. J.* **339**, 1156 (1989)] estimated that hydrogen burning started $(40 \pm 10) \times 10^{6}$ years after this time.
17. P. Demarque and J. R. Percy, *Astrophys. J.* **140**, 541 (1964).
18. Rotationally induced mixing was considered by B. Chaboyer, P. Demarque, D. B. Guenther, and M. H. Pinsonneault [*Astrophys. J.* **446**, 435 (1995)] and by O. Richard, S. Vauclair, C. Charbonnel, and W. A. Dziembowski [*Astron. Astrophys.*, in press]. Simple models of penetration beneath the convection zone predict a region of nearly adiabatic stratification, followed by a sharp transition to radiative transport [J. H. M. M. Schmitt, R. Rosner, H. U. Bohn, *Astrophys. J.* **282**, 316 (1984); J.-P. Zahn, *Astron. Astrophys.* **252**, 179 (1991)]. The extent of penetration in such simple models has been constrained to a small fraction of a pressure scale height by helioseismic analyses [S. Basu, H. M. Antia, D. Narasimha, *Mon. Not. R. Astron. Soc.* **267**, 209 (1994); M. J. P. F. G. Monteiro, J. Christensen-Dalsgaard, M. J. Thompson, *Astron. Astrophys.* **283**, 247 (1994); I. W. Roxburgh and S. V. Vorontsov, *Mon. Not. R. Astron. Soc.* **268**, 880 (1994)]. Beyond the region of penetration, which is certainly fully mixed, additional mixing might be caused by gravity waves induced by the penetration.
19. The turbulent pressure is given by $p_{\rm turb} \simeq \overline{\rho w^2}$, where w is the vertical component of the convective velocity and the overbar denotes an average. Mixing-length models with turbulent pressure were computed by N. J. Balmforth [*Mon. Not. R. Astron. Soc.* **255**, 603 (1992)]. Hydrodynamical simulations confirm the importance of $p_{\rm turb}$ in the uppermost parts of the convection zone. Significant uncertainties also arise from the treatment of the convective flux (*9*).
20. A mass loss of $0.1M_{\odot}$ during the early parts of the main-sequence phase has been suggested to explain the solar surface lithium depletion [A. I. Boothroyd, I.-J. Sackmann, W. A. Fowler, *Astrophys. J.* **377**, 318 (1991); J. A. Guzik and A. N. Cox, *ibid.* **448**, 905 (1995).
21. B. Chaboyer, P. Demarque, M. H. Pinsonneault, *Astrophys. J.* **441**, 865 (1995), and references therein. For a review of the solar lithium problem, see G. Michaud and P. Charbonneau, *Space Sci. Rev.* **57**, 1 (1990).
22. The model used the OPAL equation of state and opacities (*34*). Nuclear reaction parameters were generally obtained from (*59*). Helium and heavy-element settling was included, using the Michaud and Proffitt coefficients (*61*). The present value of $Z_{\odot}/X_{\odot}$ is 0.0245, and the age of the present sun was assumed to be 4.6 billion years. The numerical error in the calculation should be substantially smaller than the physical effects investigated. The present code has been tested against several others, using simplified but precisely defined physics [M. Gabriel, in *Challenges to Theories of the Structure of Moderate-Mass Stars*, vol. 388 of *Lecture Notes in Physics*, D. O. Gough and J. Toomre, Eds. (Springer, Heidelberg, 1991), p. 51; J. Christensen-Dalsgaard and J. Reiter, in *GONG '94: Helio- and Astero-seismology from Earth and Space*, R. K. Ulrich, E. J. Rhodes Jr., W. Däppen, Eds. (ASP Conf. Ser. 76, Astronomical Society of the Pacific, San Francisco, 1995), p. 136]. These and other tests indicate that the numerical error in the models is below 0.005%.
23. D. O. Gough, J. W. Leibacher, P. H. Scherrer, J. Toomre, *Science* **272**, 1281 (1996).
24. D. O. Gough *et al.*, *ibid.*, p. 1296.
25. Nonadiabatic frequency calculations were carried out by, for example, J. Christensen-Dalsgaard and S. Frandsen [*Sol. Phys.* **82**, 165 (1983)]; Cox, Guzik, and Kidman (*60*); N. J. Balmforth [*Mon. Not. R. Astron. Soc.* **255**, 632 (1992)]; and D. B. Guenther [*Astrophys. J.* **422**, 400 (1994)]. Turbulent pressure and convection introduce additional uncertainties (*19*).
26. J. Christensen-Dalsgaard and D. J. Mullan, *Mon. Not. R. Astron. Soc.* **270**, 921 (1994).
27. The mode inertia is defined by $E_{n\ell} = \int_V \rho |\delta \mathbf{r}|^2 dV$, where $\delta \mathbf{r}$ is the displacement associated with the oscillation, suitably normalized at the surface, and integration is over the volume V of the star. The frequency change associated with a near-surface modification is proportional to $E_{n\ell}{}^{-1}$ [J. Christensen-Dalsgaard and G. Berthomieu, in *Solar Interior and Atmosphere*, A. N. Cox, W. C. Livingston, M. Matthews, Eds. (Space Science Ser., Univ. of Arizona Press, Tucson, 1991), p. 401].
28. For modes of degree beyond the range covered by GONG, the ℓ-dependence of the near-surface effects becomes significant. D. O. Gough and S. V. Vorontsov, *Mon. Not. R. Astron. Soc.* **273**, 573 (1995); H. M. Antia, *ibid.* **274**, 499 (1995).
29. The plasma is still ideal as long as the underlying microphysics does not contain dynamical interactions. The "particles," however, can be classical or quantum, material or photonic.
30. In the solar interior, the ratio between Coulomb and kinetic energy is generally small (typically $\simeq 0.1$), although it reaches ~ 0.4 in the second helium ionization zone.
31. Such equations of state are based on a model for the free energy of the plasma, incorporating approximate statistical-mechanical models. The ionization equilibria are obtained by searching for the minimum of the free energy under the stoichiometric constraints of the reactions considered. The procedure guarantees thermodynamic consistency.
32. Here the only nonideal effect is a simple prescription to ensure full ionization in stellar cores. P. P. Eggleton, J. Faulkner, B. P. Flannery, *Astron. Astrophys.* **23**, 325 (1973).
33. D. G. Hummer and D. M. Mihalas, *Astrophys. J.* **331**, 794 (1988); D. M. Mihalas, W. Däppen, D. G. Hummer, *ibid.*, p. 815; W. Däppen, D. M. Mihalas, D. G. Hummer, B. W. Mihalas, *ibid.* **332**, 261 (1988).
34. See (*62*); F. J. Rogers and C. A. Iglesias, *Astrophys. J.* **401**, 361 (1992). As part of the OPAL project, a physical-picture equation of state suitable for stellar models was developed [F. J. Rogers, *Astrophys. J.* **310**, 723 (1986), and references therein; ———, F. J. Swenson, C. A. Iglesias, *ibid.* **456**, 902 (1996)]. For general literature on the physical picture, see W. Ebeling, A. Förster, V. E. Fortov, V. K. Gryaznov, A. Ya. Polishchuk, *Thermodynamic Properties of Hot Dense Plasmas* (Teubner, Stuttgart, 1991).
35. The physical picture has the power to avoid divergent internal partition functions of bound systems (atoms and ions), a problem that has always plagued the chemical picture.
36. J. Christensen-Dalsgaard and W. Däppen, *Astron. Astrophys. Rev.* **4**, 267 (1992).
37. Recombination to He^{+} ions at the solar center may be allowed. The maximum He^{+}/He^{++} is ~ 0.30 (*36*). However, there are mechanisms acting to destroy He^{+} ions, and helium may be virtually fully ionized in the solar core.
38. The effect would be even more prominent in the hydrogen ionization zone; however, there the uncertainty in the treatment of convection precludes practical applications.
39. For the helium-abundance determination, see S. V. Vorontsov, V. A. Baturin, A. A. Pamyatnykh, *Nature* **349**, 49 (1991); A. G. Kosovichev *et al.*, *Mon. Not. R. Astron. Soc.* **259**, 536 (1992); H. M. Antia and S. Basu, *Astrophys. J.* **426**, 801 (1994); A. G. Kosovichev, in *GONG '94: Helio- and Astero-seismology from Earth and Space*, R. K. Ulrich, E. J. Rhodes Jr., W. Däppen, Eds. (ASP Conf. Ser. 76, Astronomical Society of the Pacific, San Francisco, 1995), p. 89; (*42*).
40. J. Christensen-Dalsgaard, W. Däppen, Y. Lebreton, *Nature* **336**, 634 (1988); V. A. Baturin, W. Däppen, X. Wang, F. Yang, in *Proceedings of the 32nd Liège International Astrophysical Colloquium*, A. Noels, M. Gabriel, N. Grevesse, P. Demarque, Eds. (Université de Liège, Liège, Belgium, 1996), p. 33.
41. F. Hill *et al.*, *Science* **272**, 1292 (1996).
42. F. Pérez Hernández and J. Christensen-Dalsgaard, *Mon. Not. R. Astron. Soc.* **269**, 475 (1994).
43. The reason MHD fits better than EFF plus Coulomb correction is not clear. Higher order Coulomb terms bring no advantage over the description involving the leading term only [S. V. Vorontsov, V. A. Baturin, A. A. Pamyatnykh, *Mon. Not. R. Astron. Soc.* **257**, 32 (1992)]. Models computed with the OPAL equation of state appear to provide a better approximation to solar conditions than do those using the MHD formulation [A. G. Kosovichev, *Adv. Space Res.* **15** (no. 7), 95 (1995); J. Christensen-Dalsgaard, *Nucl. Phys. B Suppl.*, M. Fatas, Ed., in press].
44. A. N. Cox, J. N. Stewart, D. D. Eilers, *Astrophys. J. Suppl. Ser.* **11**, 1 (1965); A. N. Cox and J. N. Stewart, *ibid.*, p. 22; *ibid.* **19**, 243 (1970); *ibid.*, p. 261; A. N. Cox and J. E. Tabor, *ibid.* **31**, 271 (1976).
45. K. Fricke, R. S. Stobie, P. A. Strittmatter, *Mon. Not. R. Astron. Soc.* **154**, 23 (1971); W. B. Stellingwerf, *Astron. J.* **83**, 1184 (1978); J. O. Petersen, *Astron. Astrophys.* **34**, 309 (1974); N. R. Simon, *Astrophys. J.* **260**, L87 (1982).

46. More complete calculations produced an increase by factors of up to 100 in the opacity of pure iron [(62); F. J. Rogers and C. A. Iglesias, *Astrophys. J. Suppl. Ser.* **79**, 507 (1992); C. A. Iglesias, F. J. Rogers, B. G. Wilson, *Astrophys. J.* **397**, 717 (1992)] at temperatures where transitions originating in the M shell of iron dominate the absorption. This huge increase in iron opacity is enough to increase the total opacity by a factor of 2 to 3.
47. The Opacity Project [M. J. Seaton, Y. Yan, D. Mihalas, A. K. Pradhan, *Mon. Not. R. Astron. Soc.* **266**, 805 (1994); M. J. Seaton, Ed., *The Opacity Project* (Institute of Physics Publ., London, 1995), vol. **1**, and references therein] is mainly an atomic physics effort; plasma effects on occupation numbers are of secondary interest.
48. For example, pulsationally inferred masses [P. Moskalik, J. R. Buchler, A. Marom, *Astrophys. J.* **385**, 685 (1992); S. M. Kanbur and N. R. Simon, *ibid.* **420**, 880 (1994); J. Christensen-Dalsgaard and J. O. Petersen, *Astron. Astrophys.* **299**, L17 (1995)].
49. See, for example, J. Christensen-Dalsgaard, T. L. Duvall, D. O. Gough, J. W. Harvey, E. J. Rhodes Jr., *Nature* **315**, 378 (1985); S. G. Korzennik and R. K. Ulrich, *Astrophys. J.* **339**, 1144 (1989).
50. Much of the improvement arose because the enhanced opacity increased the depth of the convection zone to match more closely an earlier helioseismic determination (7). However, calculations using the new OPAL opacities and the physical-picture equation of state were able to bring the calculated value much closer to the observation [D. B. Guenther, P. Demarque, Y.-C. Kim, M. H. Pinsonneault, *Astrophys. J.* **387**, 372 (1992); J. N. Bahcall and M. H. Pinsonneault, *Rev. Mod. Phys.* **64**, 885 (1992); J. A. Guzik and A. N. Cox, *Astrophys. J.* **411**, 394 (1993)]. The inclusion of element settling in the models largely explains the residual difference.
51. Simple scaling arguments (5) show that the luminosity is inversely proportional to opacity and increases as a high power of the mean molecular weight μ. Thus, to compensate for the increase in opacity, an increase in μ, and hence in Y, is required [V. A. Baturin and S. V. Ajukov, *Astron. Rep.* **37**, 489 (1995)].
52. V. N. Tsytovich, R. Bingham, U. de Angelis, A. Forlani, M. R. Occorsio, *Astropart. Phys.*, in press.
53. Such improvement in helioseismic inversion was first noted by J. Christensen-Dalsgaard, C. R. Proffitt, and M. J. Thompson [*Astrophys. J.* **403**, L75 (1993)].
54. A. G. Kosovichev, in *The Sun and Beyond: 2e Rencontres du Vietnam*, L. M. Celnikier, Ed. (Editions Frontières, Gif sur Yvette, France, in press). For a recent review, see R. S. Raghavan, *Science* **267**, 45 (1995).
55. J. N. Bahcall and H. A. Bethe, *Phys. Rev. Lett.* **65**, 2233 (1990); J. N. Bahcall, *Phys. Lett. B* **33**, 276 (1994).
56. The helioseismic inferences constrain the solar pressure, density, and sound speed. With no further constraints, this leaves considerable freedom for the temperature and composition profile and hence for the neutrinos. Note, for example, that for a fully ionized ideal gas, $c^2 \propto T/\mu$; hence, T/μ is constrained, but T and μ separately are not [H. M. Antia and S. M. Chitre, *Astrophys. J.* **442**, 434 (1995)]. Models can be found that agree with both the helioseismic data and the ^{37}Cl neutrino detections; however, the internal opacity would have to be substantially reduced in such models.
57. T. M. Brown, *Annu. Rev. Astron. Astrophys.* **32**, 37 (1994).
58. V. Canuto and I. Mazzitelli, *Astrophys. J.* **370**, 295 (1991).
59. J. N. Bahcall and M. H. Pinsonneault, *Rev. Mod. Phys.* **67**, 781 (1995).
60. A. N. Cox, J. A. Guzik, R. B. Kidman, *Astrophys. J.* **342**, 1187 (1989).
61. G. Michaud and C. R. Proffitt, in *Inside the Stars*, A. Baglin and W. W. Weiss, Eds. (IAU Colloq. 137, ASP Conf. Ser. 40, Astronomical Society of the Pacific, San Francisco, 1993), p. 246.
62. C. A. Iglesias and F. J. Rogers, *Astrophys. J.* **371**, L73 (1991).
63. D. O. Gough and J. Toomre, *Annu. Rev. Astron. Astrophys.* **29**, 627 (1991).
64. S. Basu and H. M. Antia, *J. Astrophys. Astron.* **15**, 143 (1994). Convection was treated using the Canuto and Mazzitelli formulation (58).
65. A. G. Kosovichev, in *Proceedings of the Fourth SOHO Workshop: Helioseismology*, J. T. Hoeksema, V. Domingo, B. Fleck, B. Battrick, Eds. (ESA SP-376, European Space Research and Technology Centre, Noordwijk, Netherlands, 1995), vol. 1, p. 165.
66. C. S. Rosenthal *et al.*, *ibid.*, vol. 2, p. 459.
67. We thank R. Trampedach for assistance with the graphics. The work reported here was supported in part by the Danish National Research Foundation through the establishment of the Theoretical Astrophysics Center and in part by grant AST-9315112 from National Science Foundation (NSF). The GONG is managed by the National Solar Observatory, a division of the National Optical Astronomy Observatories, operated by Association of Universities for Research in Astronomy under a cooperative agreement with NSF. The data were acquired by instruments operated by the Big Bear Solar Observatory, High Altitude Observatory, Learmonth Solar Observatory, Udaipur Solar Observatory, Instituto de Astrofísica de Canarias, and Cerro Tololo Interamerican Observatory.

18 March 1996; accepted 10 May 1996

The Solar Acoustic Spectrum and Eigenmode Parameters

F. Hill, P. B. Stark, R. T. Stebbins, E. R. Anderson, H. M. Antia, T. M. Brown, T. L. Duvall Jr., D. A. Haber, J. W. Harvey, D. H. Hathaway, R. Howe, R. P. Hubbard, H. P. Jones, J. R. Kennedy, S. G. Korzennik, A. G. Kosovichev, J. W. Leibacher, K. G. Libbrecht, J. A. Pintar, E. J. Rhodes Jr., J. Schou, M. J. Thompson, S. Tomczyk, C. G. Toner, R. Toussaint, W. E. Williams

The Global Oscillation Network Group (GONG) project estimates the frequencies, amplitudes, and linewidths of more than 250,000 acoustic resonances of the sun from data sets lasting 36 days. The frequency resolution of a single data set is 0.321 microhertz. For frequencies averaged over the azimuthal order m, the median formal error is 0.044 microhertz, and the associated median fractional error is 1.6×10^{-5}. For a 3-year data set, the fractional error is expected to be 3×10^{-6}. The GONG m-averaged frequency measurements differ from other helioseismic data sets by 0.03 to 0.08 microhertz. The differences arise from a combination of systematic errors, random errors, and possible changes in solar structure.

Several million resonant acoustic normal modes (eigenmodes) of the sun are excited stochastically in the subsurface turbulent layer. The frequencies ν, amplitudes A, and characteristic widths Γ of such modes, as a function of radial order n, spherical harmonic degree ℓ, and azimuthal order m, form the basic data from which helioseismic inferences about the solar interior are drawn. The GONG project currently estimates these eigenspectral parameters for about 250,000 normal modes every 36 days, with the potential to estimate parameters for more than one million modes. Here we discuss solar oscillation spectra and random and systematic errors in the estimated mode parameters and compare GONG mode frequency estimates to those derived from three other experiments.

The amplitudes of solar oscillations are sufficiently small that linear oscillation theory is an excellent approximation. Nonetheless, there are numerous statistical problems in estimating the mode parameters from the surface motions of the sun as observed by the GONG instruments. These problems include estimating the geometry of the images of the solar disk, estimating the modulation transfer function (MTF) of the instrument and atmosphere, estimating systematic and stochastic components of the observational noise, optimally combining observations obtained at different sites into coherent time series, dealing with missing observations, and estimating parameters of a three-dimensional power spectrum and their errors and covariances. Because we observe only a portion of one side of the sun, some power leaks across spatial frequencies; this leakage makes it difficult to separate modes and distinguish splitting caused by the solar structure from that of artifacts of the observation and reduction process. The sun changes on time scales of 1 month, so common statistical prescriptions, based on frequency resolution and variance, for partitioning the years of data into shorter time series and combining their spectra do not apply directly; other methods are necessary. Similarly, the stochastic nature of the excitation process could be exploited to improve eigenspectral estimates, and statistical properties of the excitation process are interesting themselves. Our knowledge of the solar interior will become more precise as improved statistical techniques, tai-